

CZECH TECHNICAL UNIVERSITY IN PRAGUE

Faculty of Mechanical Engineering

Bachelor Thesis



Daniel Camilo Mora Sierra

**Determination of Influence of a Spoiler and a Flap on
Standard Airfoils**

Department of Fluid Dynamics and Thermodynamics

Thesis supervisor: Ing. Vít Štorch

Study program: Theoretical Fundamentals of Mechanical
Engineering

2015

I owe my deepest gratitude to Ing. Vít Štorch for his sincere advice, guidance, patience and support throughout the development and writing process of this work. I would also like to thank the staff of the Department of Fluid Dynamics and Thermodynamics of the Czech Technical University in Prague for all the help and collaboration provided for the realization of this bachelor thesis.

This thesis is dedicated to my beloved mother, who has always striven to give me the best regardless of what it might take, to my beloved brothers, who have been on my side from the very beginning and to my beloved friends.

SOLEMN DECLARATION

I declare herewith that this bachelor thesis is my own work and I carried it out independently. I only used the cited sources, literature, Ing. Vít Štorch's guidance and other professional sources.

In Prague, date

Signature

Anotace

Jméno Autora: Daniel Camilo Mora Sierra

Název bakalářské práce: Zkoumání vlivu spoileru a klapky na standardní profily

Anglický název: Determination of Influence of a Spoiler and a Flap on Standard Airfoils

Rok: 2015

Studijní program: Teoretický základ strojního inženýrství

Obor: bez oboru

Ústav: Ústav mechaniky tekutin a termodynamiky

Vedoucí bakalářské práce: Ing. Vít Štorch

Bibliografické údaje: počet stran: 28
počet obrázků: 35
počet tabulek: 0
počet příloh: 0

Klíčová slova: Klapka, spoiler, odpor, vztlak, koeficient odporu, koeficient vztlaku, profil, aerodynamika, křídlo, konečné křídlo, nekonečné křídlo, polára, vztlaková čára, odporová čára, aerodynamický tunel, výchylka, letoun, Eppler 1230, R1145MS.

Keywords: Flap, spoiler, drag, lift, drag coefficient, lift coefficient, airfoil, aerodynamics, wing, infinite wing, finite wing, drag polar, lift curve, drag curve, wind tunnel, deflection, aircraft, Eppler 1230, R1145MS.

Abstrakt: Klapky a spoilery jsou základní součásti mechanizace křídla, které umožňují zvyšovat jeho účinnost a použitelnost během letu. Cílem bakalářské práce je zkoumat vliv spoileru na profil Eppler 1230 a klapky na profil R1145MS. Jsou diskutovány základní geometrické a aerodynamické vlastnosti křídla nutné pro pochopení vlivu klapky a spoilerů. Konečné výsledky jsou získány měřením v aerodynamickém tunelu.

Abstract: Flaps and spoilers are elemental mechanization components of a wing that help the purpose of making it more efficient and suitable during flight. The goal of this bachelor thesis is to determine the influence of a spoiler on an Eppler 1230 airfoil and of a flap on R1145MS airfoil. All the basic geometry and aerodynamics of a wing necessary to comprehend the effects of flaps and spoilers are being discussed. The final results are obtained by performing a wind tunnel measurement.

LIST OF CONTENTS

LIST OF FIGURES	VIII
NOMENCLATURE.....	X
1. INTRODUCTION	1
2. GEOMETRY OF A WING	2
2.1 AIRFOIL NOMENCLATURE	2
2.2 WING PLANFORM	2
2.3 ASPECT RATIO	3
2.4 TAPER.....	4
2.5 SWEEP	5
2.6 TWIST.....	5
3. AERODYNAMICS OF A WING.....	6
3.1 LIFT.....	6
3.1.1 “Kutta-Joukowski” Theorem and the generation of lift.....	6
3.2 DRAG	7
3.2.1 Types of drag	8
3.3 DRAG AND LIFT COEFFICIENTS.....	8
3.4 AERODYNAMIC CURVES	9
4. MECHANIZATION OF A WING	11
4.1 FLAPS	11
4.1.1 Trailing-Edge Flaps	12
4.1.2 Leading-Edge Flaps.....	14
4.2 SPOILERS.....	15
5. MEASUREMENT	17
5.1 MEASUREMENT SET-UP	17
5.2 MEASUREMENT RESULTS.....	20
6. ANALYSIS AND DISCUSSION.....	24
7. CONCLUSION	26
8. BIBLIOGRAPHY.....	27

LIST OF FIGURES

FIG. 2-1 AIRFOIL DESCRIPTION. REDRAWN BASED ON: [2]	2
FIG. 2-2 WING PLANFORM TYPES	3
FIG. 2-3 GENERATION OF WING TIP VORTICES. REDRAWN BASED ON: [2] [3]	3
FIG. 2-4 ASPECT RATIO	4
FIG. 2-5 TAPER IN AIRCRAFT WINGS. REDRAWN BASED ON: [3]	4
FIG. 2-6 WING SWEEP ANGLE. REDRAWN BASED ON: [3] [6]	5
FIG. 2-7 WING TWIST. REDRAWN ACCORDING TO: [1]	5
FIG. 3-1 MOMENT AND DECOMPOSITION OF THE TOTAL AERODYNAMIC FORCE OVER AN AIRFOIL. TAKEN FROM: [5]	6
FIG. 3-2 CIRCULATION AROUND A LIFTING AIRFOIL. TAKEN FROM: [15]	7
FIG. 3-3 SKETCH OF A TYPICAL LIFT CURVE. MODIFIED FROM: [5]	9
FIG. 3-4 SKETCH OF A GENERIC DRAG CURVE. TAKEN FROM: [14]	10
FIG. 3-5 DRAG POLAR OF A NACA-0009 9.0% SMOOTHED (N0009SM-IL) FOR THE REYNOLDS NUMBER $5 \cdot 10^4$, 10^5 , $2 \cdot 10^5$, $5 \cdot 10^5$ AND 10^6 . TAKEN FROM [19]	10
FIG. 4-1 TRAILING EDGE BASIC TYPES OF FLAPS. TAKEN FROM [3]	12
FIG. 4-2 EFFECT OF TE FLAP DEFLECTION ON LIFT CURVE. TAKEN FROM [12]	13
FIG. 4-3 POSITION ANGLE [12]	13
FIG. 4-4 LEADING EDGE FLAPS. TAKEN FROM [3]	14
FIG. 4-5 EFFECT OF LE FLAP DEFLECTION ON LIFT CURVE. MODIFIED FROM [8]	15
FIG. 4-6 SPOILER'S AERODYNAMIC FUNCTION. TAKEN FROM [18]	15
FIG. 4-7 VERTICALLY EXTENDED SPOILER. TAKEN FROM [3]	16
FIG. 5-1 CROSS SECTION OF THE WIND TUNNEL'S TEST SECTION	17
FIG. 5-2 R1145MS FLAPPED AIRFOIL IN THE WIND TUNNEL TEST SECTION.	17
FIG. 5-3 EPPLER 1230 AIRFOIL WITH SPOILER 3 IN THE WIND TUNNEL TEST SECTION.....	17
FIG. 5-4 SPOILERS IMPLEMENTED ON THE EPPLER 1230 AIRFOIL	18
FIG. 5-5 MEASURING MODULES AND NI COMPACTDAQ4-SLOT USB CHASSIS	18
FIG. 5-6 a) EPPLER 1230, b) R1145MS, c) R1145MS FLAPPED.....	19
FIG. 5-7 LIFT CURVE R1145MS AIRFOIL AT REYNOLDS: A) 233000 AND B) 335000	20
FIG. 5-8 DRAG CURVE R1145MS AIRFOIL AT REYNOLDS: A) 233000 AND B) 335000.....	20
FIG. 5-9 DRAG POLAR R1145MS AIRFOIL AT REYNOLDS: A) 233000 AND B) 335000	21

FIG. 5-10 MOMENT CURVE R1145MS AIRFOIL AT REYNOLDS: A) 233000 AND B) 335000	21
FIG. 5-11 LIFT CURVE EPPLER 1230 AIRFOIL AT REYNOLDS: A) 233000 AND B) 335000	22
FIG. 5-12 DRAG CURVE EPPLER 1230AIRFOIL AT REYNOLDS: A) 233000 AND B) 335000	22
FIG. 5-13 DRAG POLAR EPPLER 1230 AIRFOIL AT REYNOLDS: A) 233000 AND B) 335000.....	23
FIG. 5-14 MOMENT CURVE EPPLER 1230 AIRFOIL AT REYNOLDS: A) 233000 AND B) 335000	23
FIG. 6-1 COMPARISON LIFT CURVE.....	24
FIG. 6-2 COMPARISON DRAG CURVE	25

NOMENCLATURE

<i>Parameter</i>	<i>Symbol</i>	<i>SI Units</i>
Airfoil drag coefficient (Profile drag)	C_d	1
Airfoil lift coefficient	C_l	1
Airfoil maximum lift coefficient	C_{lmax}	1
Angle of attack	α	°
Aspect ratio	AR	1
Chord	c	m
Circulation	Γ	$m^2.s^{-1}$
Drag	D	N
Drag coefficient	C_D	1
Drag per-unit-span	D'	$N.m^{-1}$
Dynamic pressure	q_∞	Pa
Free-stream density	ρ_∞	$Kg.m^{-3}$
Free-stream Mach number	M_∞	1
Free-stream velocity	V_∞	$m.s^{-1}$
Gain in lift at a given angle of attack	ΔC_l	1
Induced drag coefficient	$C_{D,i}$	1
Lift	L	N

Lift coefficient	C_L	1
Lift curve slope	a_0	$1/^\circ$
Lift per-unit-span	L'	$N.m^{-1}$
Lift-to-Drag ratio	L/D	1
Maximum lift coefficient	C_{Lmax}	1
Pitching moment	M	Nm
Pitching Moment at quarter chord	$M_{c/4}$	Nm
Pressure drag due to flow separation coefficient	$C_{d,p}$	1
Quarter chord	$c/4$	m
Reynolds number	Re	1
Skin-friction drag coefficient	$C_{d,f}$	1
Span efficiency factor	e	1
Stall angle of attack	α_{stall}	$^\circ$
Sweep angle	Λ	$^\circ$
Taper ratio	λ	1
Total aerodynamic force over a wing's surface	R	N
Twist angle	θ	$^\circ$
Velocity around a close curve in the flow	V	$m.s^{-1}$
Velocity parallel to the leading edge	$V_{ }$	$m.s^{-1}$
Velocity perpendicular to the leading edge	V_{\perp}	$m.s^{-1}$

Wing planform area	S	m^2
Wing root chord	c_{root}	m
Wing span	b	m
Wing tip chord	c_{tip}	m
Zero-lift angle of attack	α_{0L}	°
Position angle	φ	°

Abbreviations

<i>Description</i>	<i>Contraction</i>
Angle of attack	<i>AoA</i>
Czech Technical University in Prague	<i>CTU</i>
Fuselage center line	<i>FCL</i>
Leading edge	<i>LE</i>
Three-Dimensional	<i>3D</i>
Trailing edge	<i>TE</i>
Two-Dimensional	<i>2D</i>

1. INTRODUCTION

Flaps and spoilers are elemental mechanization components of a wing that help the purpose of making it more efficient and suitable during flight, i.e., for landing, taking-off and roll-controlling. The Goal of this bachelor thesis is to determine the influence of both flaps and spoilers on the Eppler 1230 and R1145MS standard airfoils. That is, it was not aspired to obtain precise results, but to observe and understand the effects these two devices generate on the airfoils.

A literature research was carried out to theoretically understand the measured results. The basic geometric properties of a wing (e.g., airfoil nomenclature, wing planform) that are closely related to the effects of the flaps and spoilers are studied. The aerodynamics of a wing is researched too. It includes the fundamental aerodynamic forces of drag and lift, an explanation of how they are generated, the respective dimensionless coefficients related to those two forces and the most commonly used graphs reflecting these properties. Up to this point, the parameters and properties of a wing affected by the use of flaps and spoilers are known. Therefore, flaps and spoilers are theoretically discussed. Their functioning, reasons to be used, effectiveness, types, effects and properties affected by their implementation are gone through.

At this point, the needed theory is acknowledged and a practical approach is aimed for. A wind tunnel experiment is carried out on the two standard airfoils to be tested. Each airfoil is intended to be tested for only one of the two devices. To be more specific, the Eppler 1230 airfoil is tested with spoilers of different sizes at the same location and the R1145MS airfoil is tested with a flap deflected to 3 different angles.

Later on the data to be obtained is processed, analyzed and discussed, so that it can be seen whether the obtained results are satisfactory or not and finally conclude the work.

The motivation for this bachelor work is to deeper understand the influence of the mechanization of a wing and to obtain results that could probably be used for further projects.

2. GEOMETRY OF A WING

2.1 Airfoil Nomenclature

An airfoil is an arbitrary cross section of a wing parallel to the vertical plane of the aircraft. The aerodynamic characteristics of a wing, e.g. the lift and drag it generates, are strongly affected by the shape of the airfoils from which it is built and by the variation of these airfoils from the wing root to the wing tip, both in shape and orientation (twist). Therefore, choosing a particular shape of airfoil for a wing helps to optimize its lift and drag characteristics to fulfill the requirements of a particular goal.

Frequently, airfoils are also called two-dimensional wings or infinite wings because wing-tip effects are neglected.

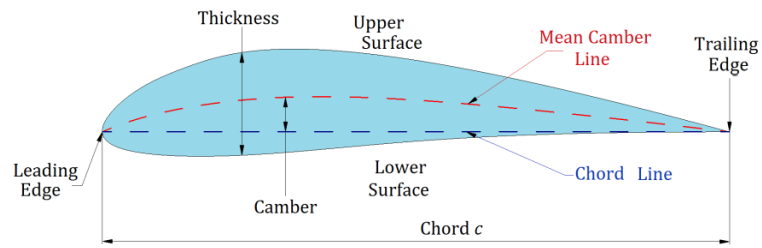


Fig. 2-1 Airfoil description. Redrawn based on: [2]

The *mean camber line* is located midway between the upper and the lower surface of the Airfoil. The *leading edge* (LE) is the furthest forward point (facing the incoming flow) of the mean camber line, while the *trailing edge* (TE) is the furthest backward point of the mean camber line. The straight line joining the LE and TE is called *chord line* and the precise distance from the LE to the TE measured along the chord line is simply called *chord* of the airfoil, designated by the symbol c . The maximum camber of an airfoil is located at a position along the chord line where the distance between the chord line and the mean camber line is maximal.

2.2 Wing Planform

The wing planform is the shape given by the projection of the wing either in top or bottom views (see Fig. 2-2). Hence, the wing planform area, S , is a measure of the total surface of this layout, including those parts which may be covered by the fuselage or the nacelles. It can be calculated as the product of the average chord and the span of the wing, b . [1] [3] [7]

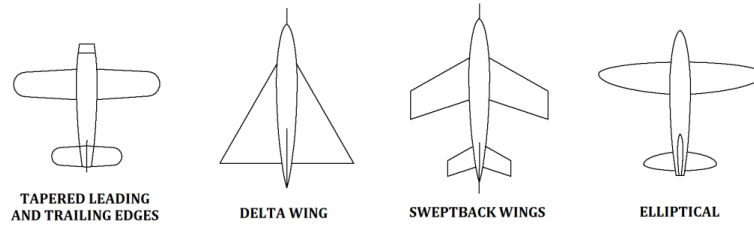


Fig. 2-2 Wing planform types

The behavior of the flow around an arbitrary wing is linked to its span. A finite wing has a 3D flow instead of the 2D flow around an airfoil.

The air flow around the wing produces a region of relatively low pressure above the wing and a region of relatively high pressure under the wing. As a result for a finite wing, the high-pressure air underneath the wing directs outboard and overflows at the tips. Regions of turbulence and thus, vortices, are formed at the tips (see Fig. 2-3). [2] [3]

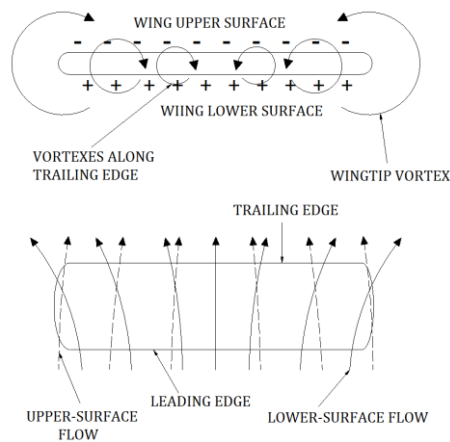


Fig. 2-3 Generation of wing tip vortices. Redrawn based on: [2] [3].

2.3 Aspect Ratio

An infinite wing would prevent the creation of wing tip vortices. However, in the real case of a finite wing the reduction of wing tip vortices can be helped by changing the aspect ratio. [3]

The Aspect Ratio, AR, is defined as the ratio of the square of the span to the wing planform area [1] [3], as follows:

$$AR = \frac{b^2}{S} \tag{2.1}$$

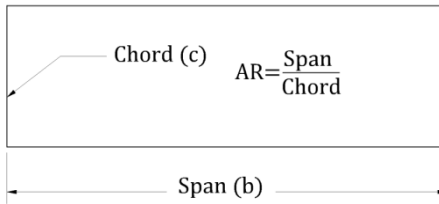


Fig. 2-4 Aspect ratio.

A high AR means long-span wing, and a low AR means either a short-span wing or a thick-chord wing. The induced drag of an aircraft is inversely dependent on the AR [6]. A large AR generates a high lift-to-drag ratio and consequently the aircraft performance is benefited in all aspects [2] [14]. On the other hand, a high AR has disadvantages as well. An increased span implies higher bending moments which must be counteracted by massive root sections due to the shorter root chord. As a consequence, an extra structural weight is generated [2] [7] [14]. Despite being less efficient than a high AR wing, a low AR wing gives more maneuverability which is crucial aerobatic airplanes and fighter aircrafts as well [7].

2.4 Taper

A tapered wing is such with one or more of its dimensions gradually decreasing from the root to the tip (see Fig. 2-5). Taper in plan and thickness is realized when both thickness and chord of the wing decrease. Taper in plan is realized when only the chord decreases along the span. Taper in thickness ratio is realized when only the thickness ratio of the wing changes along the span. [3]

A tapered wing comes together with several advantages. The load along the wing span is adjusted so the wing tips load is reduced and high bending moments are not generated. Lift is adjusted along the span in order to reduce drag [7].

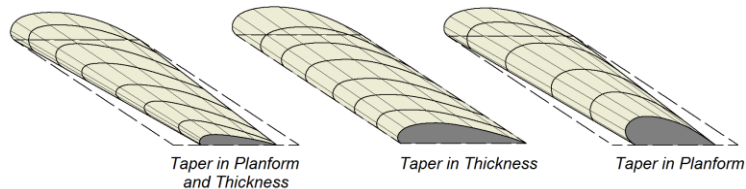


Fig. 2-5 Taper in aircraft wings. Redrawn based on: [3].

The taper ratio, λ , is the ratio of the wing tip chord to the wing root chord [1] [3], and can be expressed as:

$$\lambda = \frac{c_{tip}}{c_{root}} \quad (2.2)$$

2.5 Sweep

A swept wing is created when the leading edge is angled either backward or forward from the fuselage. The **sweep angle**, Λ , is usually defined as the angle between the quarter-chord line of the wing, measured from the leading edge and a perpendicular line to the longitudinal axis of the aircraft, as shown in **Fig. 2-6**. [1] [3]

A backward-sweep brings out several positive effects for a wing. Drag at speeds near or above the speed of sound is reduced, therefore the power required to sustain cruise speeds is reduced [3] [7]. A backward-sweep allows a more stable wing, which is desirable for passenger airplanes [3] [7]. Some negative effects such as the reduction in the wing lift curve slope and the reduction in C_{Lmax} and tip stall are generated too [8]. On the other hand, forward-sweep is not commonly used. Although it increases maneuverability, the wing is less stable [7].

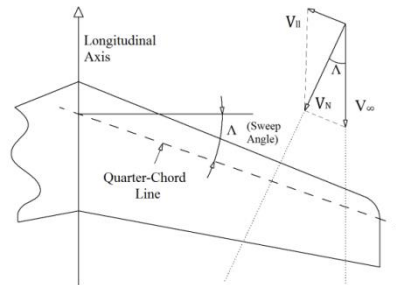


Fig. 2-6 Wing sweep angle. Redrawn based on: [3] [6]

2.6 Twist

A wing twist is an aerodynamic feature which aims to tailor the lift distribution on the wing. A wing is twisted when the wing tip is nosed down in relation to the wing root (**Fig. 2-7**), washout. In other words, the wing tip is at a lower AoA than the wing root. A twist causes the wing tip to be unloaded and to be the last part of the wing surface to stall. In this case the ailerons are still effective and so the pilot has roll control over the airplane and can prevent an uncontrolled stall spin. In the case the tip stalled first, the pilot would not have roll control at stall, and the airplane would spin. On the other hand, a wash-in is the upward-twist of the wing tip [1] [7].

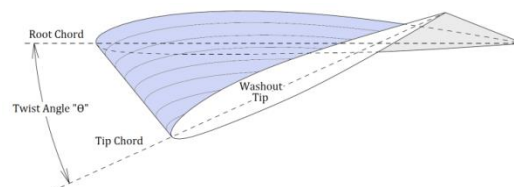


Fig. 2-7 Wing twist. Redrawn according to: [1]

3. AERODYNAMICS OF A WING

3.1 Lift

Lift is the force generated by an aircraft to overcome the force of gravity and fly in the air. It is the perpendicular-to-the-relative-wind component of the total aerodynamic force created over the wing surface due to pressure (acts locally perpendicular to the surfaces) and shear stress distributions (acts locally parallel to the surfaces) [5] [14]. There are several theories giving explanation on how this Force is generated, such as the Newton's third law of motion and the Bernoulli's principle. However, it will only be discussed the well-known "Kutta-Joukowski Theorem". It must be kept in mind that the source of lift is the net imbalance of the surface pressure distribution, and the Kutta-Joukowski Theorem is an alternative way of expressing this phenomenon (for the analysis of inviscid, incompressible flow) [15].

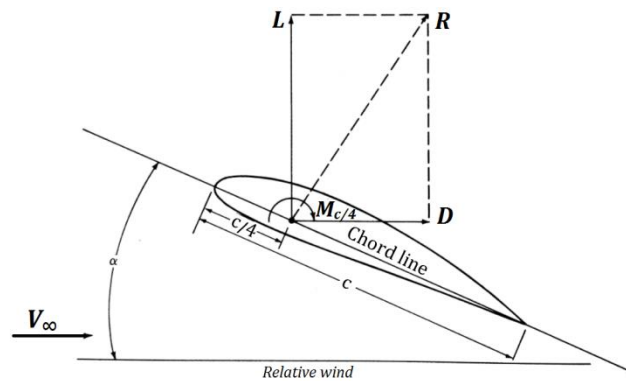


Fig. 3-1 Moment and decomposition of the total aerodynamic force over an airfoil. Taken from: [5]

3.1.1 "Kutta-Joukowski" Theorem and the generation of lift

Circulation, a fundamental tool for this theorem is defined as:

$$\Gamma \equiv - \oint_C \mathbf{v} \cdot d\mathbf{s} \quad (3.1)[15]$$

Circulation is the negative of the line integral of velocity around a closed curve in the flow. This kinematic property depends only upon the velocity field and chosen curve C . The negative sign is used in order to express the positive circulatory flow as clockwise. Note that the existence of circulation in a flow field means a finite line

integral in equation (3.1), and not necessarily that fluid particles are rotating within this flow field. [15]

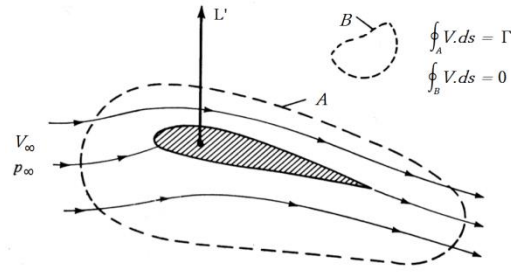


Fig. 3-2 Circulation around a lifting airfoil. Taken from: [15]

Let us consider an incompressible flow over an airfoil, as shown in Fig. 3-2. In the case that such an airfoil, enclosed by an arbitrary curve A in the flow, is producing lift, the circulation

$$\Gamma \equiv - \oint_A \mathbf{V} \cdot d\mathbf{s}$$

is finite. As a consequence, the lift per-unit-span L' on the airfoil will be given by the *Kutta-Joukowski theorem*,

$$L' = \rho_{\infty} V_{\infty} \Gamma \tag{3.2}[12][15][16]$$

where ρ_{∞} is the free-stream density and V_{∞} is the freestream velocity.

The *Kutta-Joukowski theorem* applies to any cylinder independent on its cross section and states that the lift per unit span on a two-dimensional body is directly proportional to the circulation around the body [10] [12] [15]. It is highly important to remark the fact that the value of Γ used in equation (3.2) has to be evaluated around a closed curve which can be arbitrary, but necessarily enclosing the body; For a curve which does not enclose the body, for instance curve B in Fig. 3-2, due to the irrotational flow outside the airfoil, the circulation is $\Gamma=0$ [15].

3.2 Drag

Drag is the second component of the already named total aerodynamic force over a wing, and it is parallel to the relative wind (see Fig. 3-1). This aerodynamic quantity plays a very important role, if not the most important role in airplane performance and design. Drag is wanted to be as little as possible, that is, to efficiently produce lift. The lift-to-drag ratio L/D is a measure of the aerodynamic efficiency of the aircraft; the higher the value of this coefficient is the more Newton's of lift are obtained per Newton of drag. [5] [14]

It is important to acknowledge that drag is harder and more tenuous to analytically predict than it is for lift. [14]

3.2.1 Types of drag

There exist several types of drag; however, they all fall in either of the two general types: **Pressure drag** and **friction drag**. The former is due to the net imbalance of surface pressure acting in the drag direction, and the latter is due to the net effect of shear stress acting in the drag direction. [14]

Let us now discuss the more specific types of drag. Note that both the physical nature of drag and its prediction are in comparison to lift more fundamentally affected by the Mach number; therefore, depending on the Mach-number regime different types of drag are generated. Nevertheless, only the subsonic-regime generated types of drag will be covered in this thesis. [14]

When considering the drag on an airfoil it is talked about **profile drag** or sometimes called **section drag**. *Profile drag* is the sum of **skin-friction drag** and **pressure drag due to flow separation**. *Skin-friction drag* is caused by the frictional shear stress acting on the surface of the airfoil and *Pressure drag due to flow separation* is generated by the net imbalance of the pressure distribution in the drag direction when the boundary layer separates from the airfoil surface. The two components of the profile drag depend on viscosity for their existence, meaning that they cannot exist in an inviscid flow. On the other hand, considering a finite wing brings out another type of drag. **Induced drag** is a pressure drag dependent on lift and caused by the induced flow or downwash associated with the wing-tip vortices; it is the undesirable but unavoidable by-product that is paid for the generation of lift. This type of drag is zero for infinite wings [5]. [3] [14] [16]

Other types of drag are: **Interference drag**, which is a pressure drag due to mutual interaction (interference) of the flow fields around each component of the airplane; **Parasite drag**, which is composed of interference drag, skin-friction drag and pressure drag due to flow separation, all over the complete airplane surface. [3] [14] [16]

3.3 Drag and Lift coefficients

One of the most important relations in applied aerodynamics regarding both drag and lift is given as follows:

$$\text{a) } L = q_{\infty} S C_L \qquad \text{b) } D = q_{\infty} S C_D \qquad \text{(3.3-a/b)[5][15]}$$

This expression, where $q_{\infty} \equiv \frac{1}{2} \rho_{\infty} V_{\infty}^2$ is the dynamic pressure, S is the wing planform area (aerodynamic surface) and C_D and C_L are the drag and lift coefficients respectively, is written for a 3D body (wing). Equation (3.3-a.b) can be rewritten in order to define the drag and lift coefficients:

$$\text{a) } C_L \equiv \frac{L}{q_\infty S} \qquad \text{b) } C_D \equiv \frac{D}{q_\infty S} \qquad \text{(3.4-a/b)[5][15]}$$

Both the drag and lift coefficients are equal to the corresponding aerodynamic force divided by both the dynamic pressure and a reference area. In the 2D case of an airfoil, the reference area $S=c(l)=c$, the indexes "L" and "D" are denoted by small letters and the drag and lift per unit span are used;

$$\text{a) } c_l \equiv \frac{L'}{q_\infty c} \qquad \text{b) } c_d \equiv \frac{D'}{q_\infty c} \qquad \text{(3.5-a/b)[5][15]}$$

These coefficients are not only a function of the AoA α , but also of the free-stream Mach number M_∞ and the Reynold's number Re ;

$$\text{a) } C_L = f_1(\alpha, M_\infty, Re) \qquad \text{b) } C_D = f_2(\alpha, M_\infty, Re) \qquad \text{(3.6-a/b)[5]}$$

3.4 Aerodynamic curves

The analysis of the properties of an aerodynamic body moving inside a flow is mainly based on the drag curve, lift curve and drag polar. These graphs are usually obtained in praxis by a wind tunnel experimental approach. This method is more reliable and closer to reality than numerical methods.

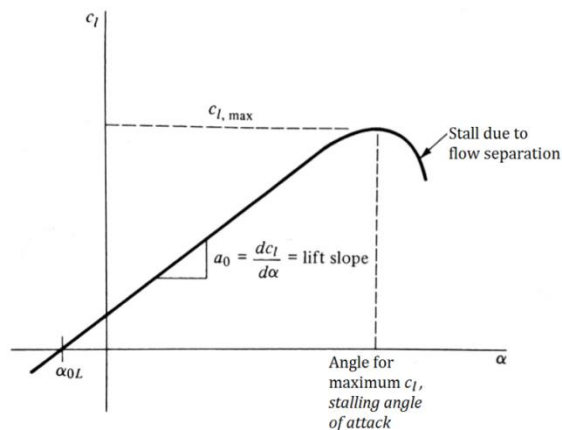


Fig. 3-3 Sketch of a typical lift curve. Modified from: [5]

A lift curve is a graph expressing the dependence of C_L to α . **Fig. 3-3** shows a sketch of this dependency for an airfoil. The slope of the linear part of the lift curve is denoted as $a_0 \equiv dc_l / d\alpha$. As it can be seen in **Fig. 3-3**,

there is still a positive c_l when $\alpha = 0$. That is, the airfoil produces lift even when being at a zero angle of attack to the free-stream. This behavior is typical of cambered airfoils. The value of α when lift is zero is called the zero-lift angle of attack α_{0L} and it can be seen in **Fig. 3-3**. Note that the lift curve for a symmetric airfoil goes through the origin. When α is increased beyond the value at which c_l reaches its maximum, c_{lmax} , the lift decreases and stall is generated.

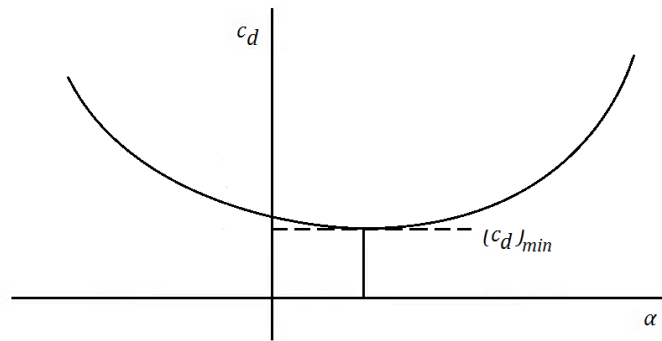


Fig. 3-4 Sketch of a generic drag curve. Taken from: [14]

A drag curve is the plot of the dependence of C_D to the AoA α . Since the lift coefficient is a linear function of the AoA, the shape of a drag curve is the same as it is for a drag polar [14]. A sketch of a generic drag curve can be seen in **Fig. 3-4**. Note that the value of $(c_d)_{min}$ is sensitive to Reynolds number and is larger at lower Reynolds numbers. The coefficient c_d is sensitive to the Reynolds number at large values of α . [14]

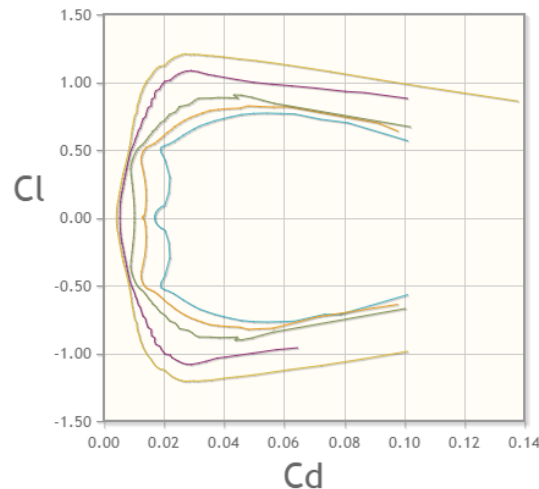


Fig. 3-5 Drag polar of a NACA-0009 9.0% smoothed (n0009sm-ii) for the Reynolds number $5 \cdot 10^4$, 10^5 , $2 \cdot 10^5$, $5 \cdot 10^5$ and 10^6 . Taken from [19]

A drag polar is simply a plot of C_D vs C_L (see **Fig. 3-5**). However, this plot is essential to the design of airplanes (performance analysis) because it basically reflects all of the aerodynamics of them [5] [14]. If the plot

is done for an infinite wing then the total coefficient of drag C_D will be equal to the coefficient of profile drag c_d ;

$$C_D = c_d = c_{d,f} + c_{d,p} \quad (3.7)[5]$$

where $c_{d,f}$ is the coefficient of skin-friction drag and $c_{d,p}$ is the Pressure drag due to flow separation. On the other hand, C_D of a finite wing includes the coefficient of induced drag $C_{D,i}$;

$$C_D = c_d + C_{D,i} \quad (3.8)[5]$$

where $C_{D,i}$ is given by:

$$C_{D,i} = \frac{C_L^2}{\pi e AR} \quad (3.9)[5]$$

In equation (3.9) AR represents the aspect ratio and e is the so called *span efficiency factor*. For elliptical planforms, $e = 1$; for all other planforms, $e < 1$. Therefore, the induced drag is a minimum for an elliptical planform [5].

4. MECHANIZATION OF A WING

4.1 Flaps

Flaps are movable surfaces on the wing or airfoil. Whenever an aircraft decreases its velocity its lift must be almost equal to its weight because the vertical acceleration is very small. For a constant wing area, according to equation (3.3-a) it can be seen that as the velocity decreases, the coefficient of lift must increase, which means that there must be an increment in the AoA. This increment may generate danger by rising close to the stall angle, or at least result in an undesirable nose-up landing attitude. A suitable alternative is a flap. [10]

Flaps are devices added to the wings of an aircraft in order to increase their lift characteristic in comparison to that of the unmodified basic airfoil. This is achieved by increasing the suction on the upper surface relative to that on the lower surface and by delaying or preventing the flow separation [8]. Their location is usually inboard on the wings' trailing edges neighboring the fuselage. However, leading edge flaps are used too. Some airplanes, such as heavy aircraft, have both LE and TE flaps, although they are usually not operated independently but in conjunction. The implementation of flaps enables landing at lower speeds and shortens the runway for both

takeoff and landing. It is necessary to clarify the fact that flaps increase drag as well (acts like a brake when the airplane rolls to stop on the landing runway) and the amount of lift generated depends on the type of flap used [3] [11].

There are several factors to be considered upon how effective flaps can be on a wing configuration. The size of the wing area affected by the flaps is one of these factors. In the case of a finite wing where the span is not only reserved for the placement of trailing edge flaps, but ailerons as well, the wing's maximum lift properties are less than those of an infinite wing. When it comes to a thin wing, any kind of flap will be less effective than it is for a thicker wing; however, a thick wing generates more drag [3].

4.1.1 Trailing-Edge Flaps

Trailing-Edge flaps are located on the rear point of the wing. By deflecting these control surfaces, the airfoil camber is increased as well as the flow acceleration on the upper surface (and overall wing circulation due to a change in the Kutta-Joukowski boundary condition at the trailing edge); that is to say, the suction on the upper surface is increased relative to that of the lower surface. As a result, the coefficient C_L is increased [8] [4].

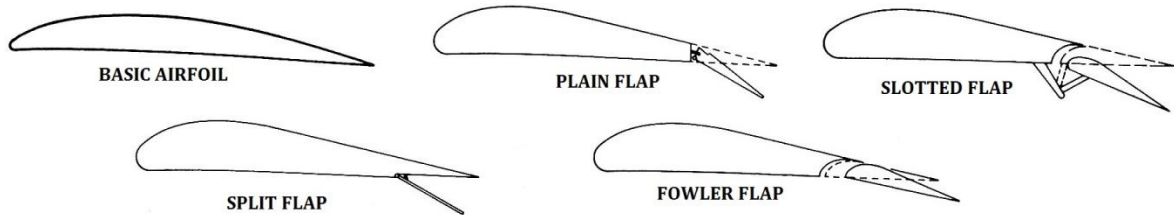


Fig. 4-1 Trailing edge basic types of flaps. Taken from [3]

As a TE flap increases the camber of the profile, its base as a high lift device can be analyzed according to the properties of a cambered airfoil. Unlike a symmetric airfoil, for a cambered profile the coefficient C_L is not zero when the AoA is zero. Therefore the angle of attack for zero lift, α_{0L} , is introduced:

$$\alpha_{0L} = -\frac{1}{\pi} \int_0^{\pi} \frac{dz}{dx} (\cos \varphi - 1) d\varphi \quad (4.1)[12]$$

In the equation (4.1) it can be seen that for the LE, where $\theta=0$, the term $(\cos \theta - 1)$ is canceled; on the other hand, its absolute value reaches maximum at the TE, where $\theta=\pi$. Therefore, the part of the mean camber line in the close neighborhood of the TE influences the most the value of α_{0L} , which is the base fact of a flap. When a part of the chord line at the TE is deflected down, the ordinate of the mean camber line is effectively made more positive, generating a more negative α_{0L} and increasing the lift at a given AoA. [12]

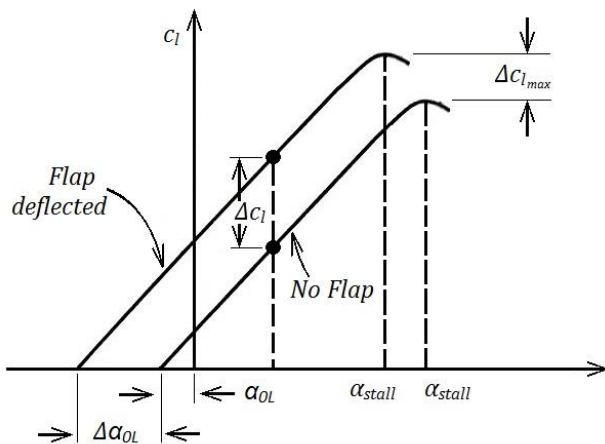


Fig. 4-2 Effect of TE flap deflection on lift curve. Taken from [12]

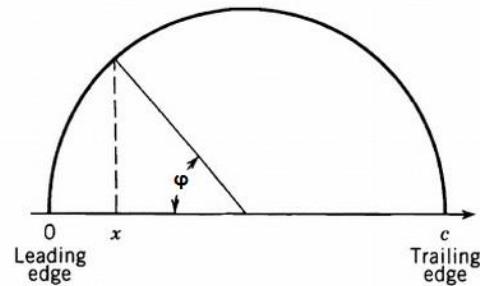


Fig. 4-3 Position angle [12]

The effects of TE flaps can be seen in **Fig. 4-2**. The negative increase in α_{OL} shifts the lift curve to the left. For every AoA below α_{stall} the airfoil generates more lift. This gain in lift for a given AoA is shown as Δc_l . The maximum lift coefficient c_{lmax} is greater; however, it happens at a lower AoA. [5] [9] [12]

Fig. 4-1 illustrates some common TE flaps. The plain flap increases lift by increasing the effective camber of the airfoil, but it is limited by the generation of drag and pitching moment. In the case of a split flap, only the bottom surface of the rear part of the airfoil is deflected downward to increase the camber. It has a higher C_{Lmax} coefficient compared to a plain flap, however, it generates more drag (reason why it is rarely used in modern airplanes) and less change in pitching moment. Slotted flaps, whether it is single-slotted, double-slotted or triple-slotted, allow high-energy air to go through the slots and up over the upper surface, modifying and stabilizing the boundary layer and delaying flow separation. Although these types of flaps generate the highest lift increment, its benefit is linked to an increased mechanical complexity. Fowler flaps increase lift based on an increase in the wing area by an aft movement before being deflected, and can be slotted to increase the beneficial effect. [9] [14]

Note the following facts: the changes on the lift curve of a wing due to the deflection of TE flaps vary depending on the type of flap used; The effectiveness of TE flaps is based upon the fact that, although the stalling angle α_{stall} is reduced, the reduction does not detract from the advantageous shift of the curve as a whole; the lift-curve slope is insignificantly affected (remains unchanged) by the TE flaps deflection; When it comes to low-speed aircraft, TE flaps can extend from the fuselage up to a 55% of the semi span of the wing. For a high speed aircraft, which has spoilers to provide more roll control, the portion of the semi span reserved for ailerons is reduced, and TE flaps can extend up to a 75% of the semi span. [5] [10] [12] [13]

Regarding flow separation, these devices themselves do not delay it neither prevent it. Instead, the increased circulation increases the suction peak at the leading edge, generating an earlier boundary-layer

separation. It can be seen in **Fig. 4-2** where the value for α_{stall} is slightly decreased [8] [2]. Nevertheless, multi-element or slotted flaps duct high pressure air from the lower to the upper surface of the flap, thus delaying boundary-layer separation (stall) to higher AoA and higher values of C_{lmax} [9] [10].

4.1.2 Leading-Edge Flaps

Leading-Edge flaps prevent flow separation by reducing the adverse pressure gradient over the top of the airfoil. Alike TE flaps, although affecting to a small extent, deflection of leading-edge flaps increases the camber of the airfoil section and thus a slight change in α_{OL} can be seen [8]. LE flaps are usually used only on large transport-category aircraft, such as the Boeing 707 and the Boeing 747 with the Krueger flaps, which need huge additional amounts of lift for landing [3]. LE flaps are usually employed over the outer half-span to reduce tip stall. The typical optimum flap deflection is between 30 and 40 degrees [8].

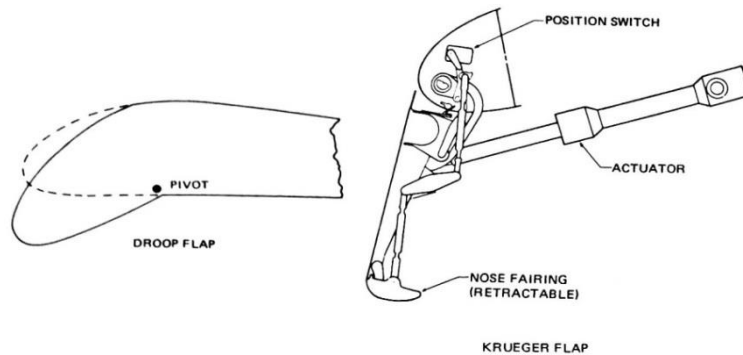


Fig. 4-4 Leading edge flaps. Taken from [3]

LE flaps can be designed in 2 basic ways; the first one consists on a wing's leading edge which can be drooped, and the second one, which was already named, on providing an extendable surface, Krueger flap, that is mounted on the lower surface of the wing. [3]

Devices at the TE are more effective than the LE devices (by about a factor of 3) because of the greater distance from the airfoil aerodynamic center (quarter chord) [10]. An airfoil equipped with leading edge devices and triple slotted TE flaps generates about the ultimate in C_{Lmax} associated with purely mechanical high lift systems. However it is also the ultimate upon mechanical complexity. [14]

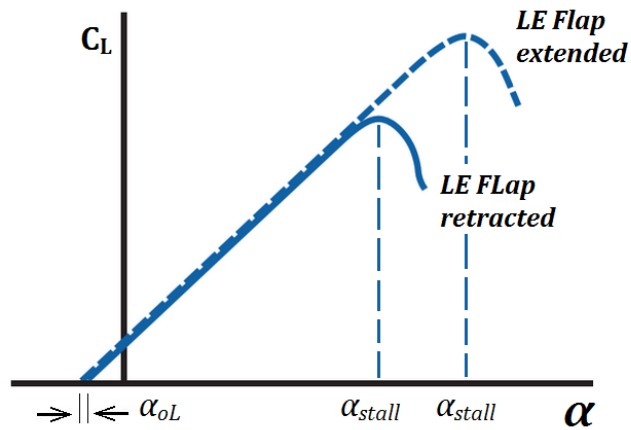


Fig. 4-5 Effect of LE flap deflection on lift curve. Modified from [8]

4.2 Spoilers

Spoilers are plate-shaped devices (control surfaces) intended to reduce lift in an aircraft. They are mounted on the upper surface of the wing and can work in two different configurations. The first and most common configuration, shown in **Fig. 4-6**, which is similar to that of a split flap, has a flat panel spoiler hinged at its forward edge and aligned with the surface of the wing. Then, the spoiler is angularly deflected and raised up to spoil the air [3]. The second configuration, which is common among sail planes, has the spoiler located inside the wing structure. The spoiler is deflected vertically from the wing to spoil the air (shown in **Fig. 4-7**) [3]. The deployment of a spoiler generates a carefully controlled stall over the part of the wing behind it, which greatly decreases lift of that wing section; In addition to the lift reduction spoilers also generate a change in pitching moment (for both airfoil characteristics and aircraft's behavior) and an increase in drag [4] [17] [18].

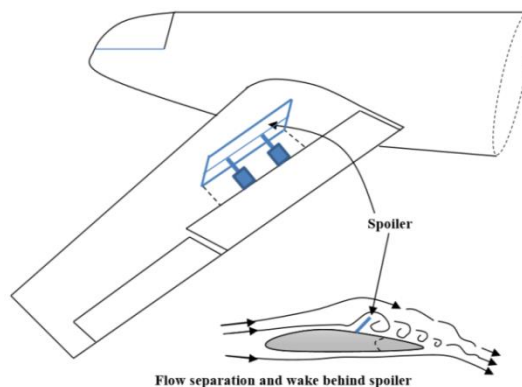


Fig. 4-6 Spoiler's aerodynamic function. Taken from [18]

Spoilers are used for several functions on an aircraft. They help to roll-control the airplane. To turn left, for instance, the spoilers on the left wing must be extended, which causes a lift decrease and a drag increase, both for this wing. Then, the left wing drops and the aircraft banks and yaws to the left. They are used as speed brakes in flight. When spoilers are symmetrically extended on both wings during flight the aircraft can be either slowed in level flight or can descend without gaining speed. They are used as lift dumpers too. By extending the spoilers on the ground, the wing's lift is reduced, which directs more portion of the aircraft's weight from the wing to the landing gear and, thus, the braking effectiveness improves (less chance for the wheels to skid); spoilers help decelerate and shorten ground runs after landing or aborted take-offs. [4] [17] [18]

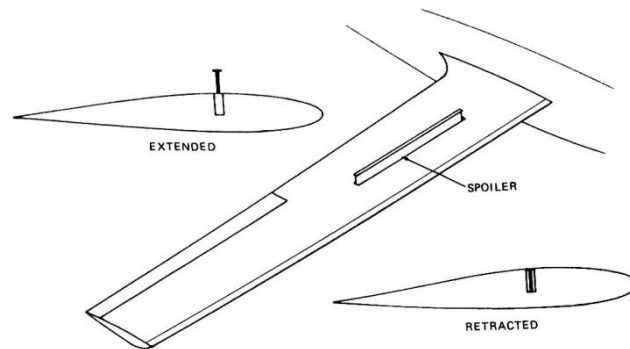


Fig. 4-7 Vertically extended spoiler. Taken from [3]

Spoilers are a mechanism that aids safe and smooth landings. However, it is not the only one helping this purpose. Airbrakes do it too. The difference between these 2 mechanisms is that the former greatly reduces lift making a moderate change in drag and the latter increases drag making a moderate change in lift. [17] [18]

The aerodynamic function of a spoiler is almost opposite to that of a high lift device (e.g., flap). When a spoiler is deflected, that is, upwards, the wing lift decreases; while the deflection of a high lift device, that is, in a downward direction, increases the wing lift. Nevertheless, both the high lift device and the spoiler increase the wing drag. [18]

The location of a spoiler on a finite wing depends upon its purpose. A spoiler for the purpose of landing deceleration must be the closest possible to the fuselage center line (FCL). On the other hand, a spoiler for the purpose of roll control should be the furthest possible to the FCL. Either a close or a far location to the FCL creates respectively small bending moment, so the structure will be lighter, and a large rolling moment. The symmetry of the spoilers on both wings, that is, equal area and distance to the FCL, guarantees straight line path during landing because yawing moments are avoided when they are deflected. [18]

5. MEASUREMENT

5.1 MEASUREMENT SET-UP

An experimental approach is chosen in order to obtain the data that will allow determining the influence of flaps and spoilers on the airfoils. The experiment was realized in a wind tunnel at the laboratories of the department of fluid dynamics and thermodynamics of CTU. It is a low Reynold's number wind tunnel (low flow rate air of 40 m/s) with an open test section and an octagonal opening (see **Fig. 5-1.**) The air blower consists of a 3.9 kW driving power and a maximum speed of 1280 rev/min [20]. The flow rate depends on the speed of the fan, which is regulated by changing the input voltage [20].

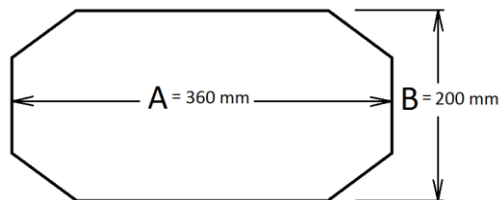


Fig. 5-1 Cross section of the wind tunnel's test section

The airfoils were placed into the test section by the use of the set-up designed in [20]. It basically consists of a frame of aluminum profiles with 4 x Zemic L6D-C3 x-3 kg load cells attached on top of it and set to measure both the lift and moment of the testing sample, and 2 x Zemic L6B-C3D-0.6 kg load cells located at $A/2$ right next to the horizontal boundary of the wind tunnel's opening. Two end plates are used to place the test sample right in the middle of the opening and to reduce the wing tip vortices. The end plates are hanged from the four load cells on top and connected to the two load cells that measure drag. For further information consult [20].

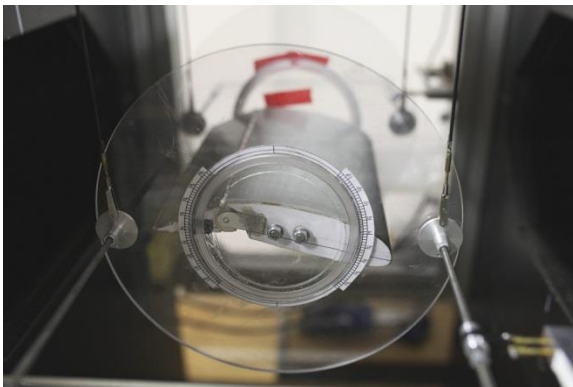


Fig. 5-2 R1145MS flapped airfoil in the wind tunnel test section.

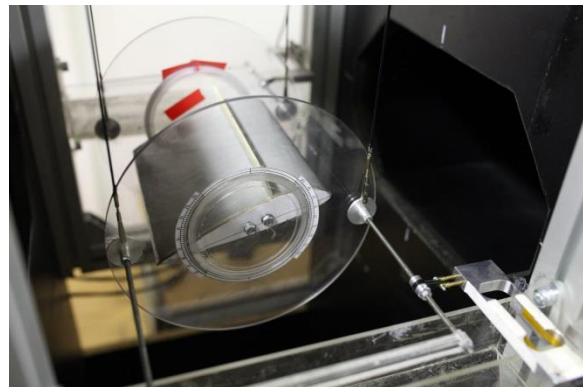


Fig. 5-3 Eppler 1230 airfoil with spoiler 3 in the wind tunnel test section.

The coordinate points of the Eppler 1230 and R1145MS airfoils were obtained from [19] and [21] respectively. The software AUTOCAD 2014 [22] was used for plotting the coordinates of the airfoil. The airfoils were cut using a hot wire foam cutter and then reinforced both on the sides with three-millimeter plywood and on the whole surface with a layer of fiberglass which also gave a smooth finish. Their chord length was 150 mm and the span length was 200 mm. A threaded rod was used for attaching the airfoils to the end plates of set-up [20] (see **Fig. 5-2** and **Fig. 5-3**).

Eppler 1230 airfoil was tested in an angle of attack range from -12 degrees up to 28 degrees by a 2-degree step at the two Reynold's numbers; a) 233000 and b) 335000. Three different vertically extended spoilers were implemented and cut from three-millimeter plywood. They extended along the span in between the side-reinforcement plywood. The vertical extension for each spoiler was constant and respectively 5 mm, 10 mm and 20 mm starting from the first one up to the third one (see **Fig. 5-4**). The measurement was initially carried out for the airfoil with no modification and subsequently for each of the spoilers attached to the airfoil.

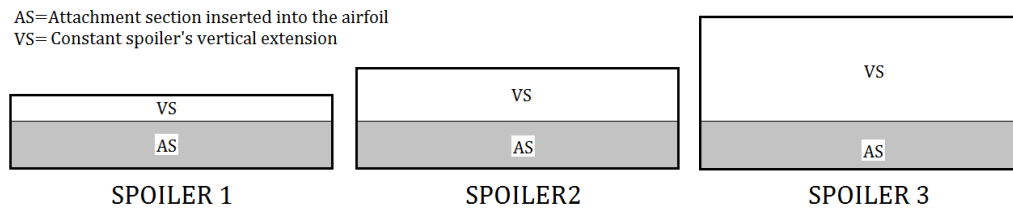


Fig. 5-4 Spoilers implemented on the Eppler 1230 airfoil

On the other hand, R1145MS airfoil was tested in an angle of attack range from -12 degrees up to 27 degrees by a 3-degree step and for the same two Reynold's number the Eppler 1230 was tested at. The measurement was initially carried out for the airfoil with no modification. Then, based on a suggestion given on [21], the airfoil was cut into a main element and a single slotted kind of TE flap. Later on, the measurement was done for the flapped airfoil for 0-degree, 10-degree, 20-degree and 30-degree deflections of the flap.



Fig. 5-5 Measuring modules and NI CompactDAQ4-Slot USB Chassis

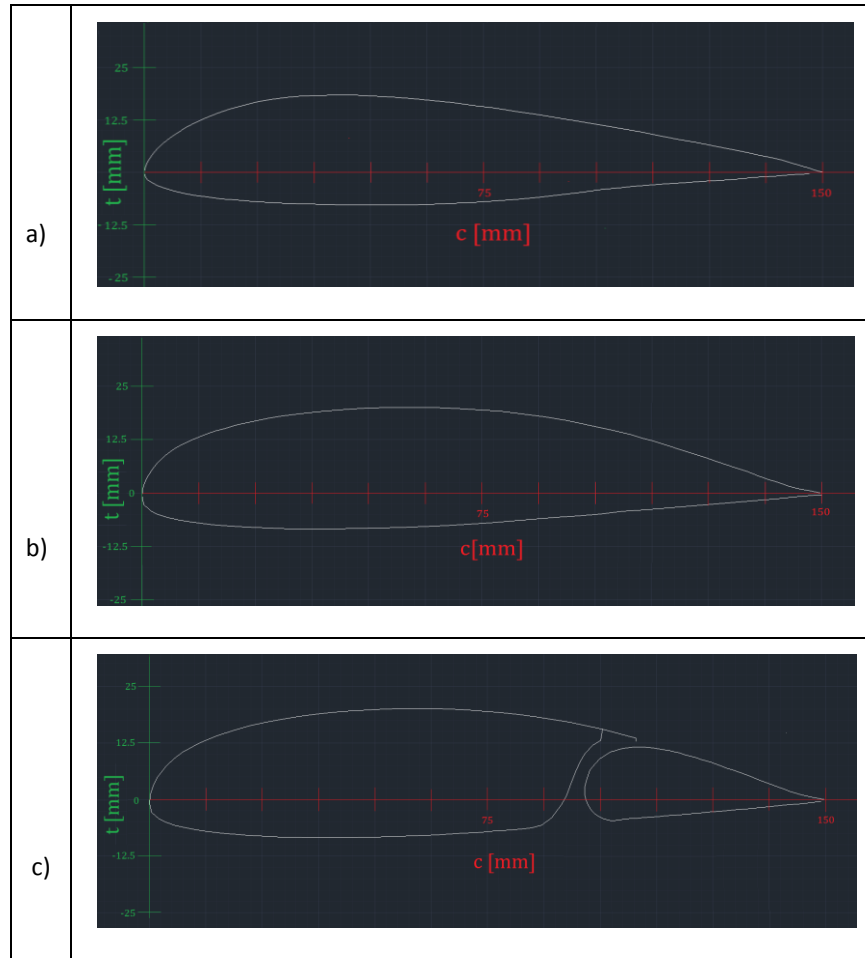


Fig. 5-6 a) Eppler 1230, b) R1145MS, c) R1145MS flapped

The data obtained from the load cells was transferred via Ethernet cables to two measuring modules inserted on a NI CompactDAQ 4-Slot USB Chassis, and then via USB cables into the pc (see Fig. 5-5). Two MATLAB [23] scripts were written for the realization of the measurement. The first one was a calibration script for the load cells, and the second one was a calculation script that returned the forces corresponding to each of the load cells for each angle of attack measured. The load cells were calibrated before the whole measurement was started. Note that the drag forces obtained from the load cells included the drag of the end plates too. Therefore, the drag of the end plates must be subtracted in order to obtain the drag force of the airfoil only. The solution was to measure with a cylinder of diameter 15,3 mm and length 200 mm. When the total drag of the plates and cylinder was obtained, the cylinder's drag was calculated by obtaining its drag coefficient from diagrams. Thus, by simply subtracting the calculated cylinder's drag from the cylinder plus end plates drag, the drag of the plates is obtained and consequently the drag of the airfoil only.

5.2 MEASUREMENT RESULTS

This chapter presents the obtained data from the measurements in a graphical form. The obtained data was plotted independently for both Reynold's numbers into the lift curve, drag curve, drag polar and moment curve.

- R1145MS:

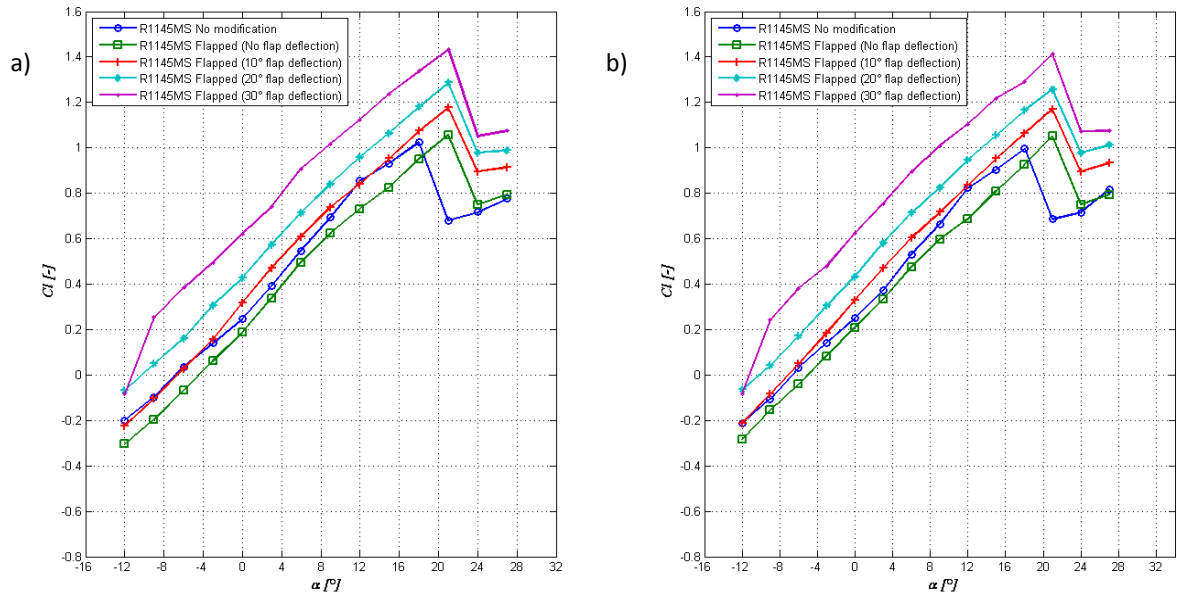


Fig. 5-7 Lift curve R1145MS airfoil at Reynolds: a) 233000 and b) 335000

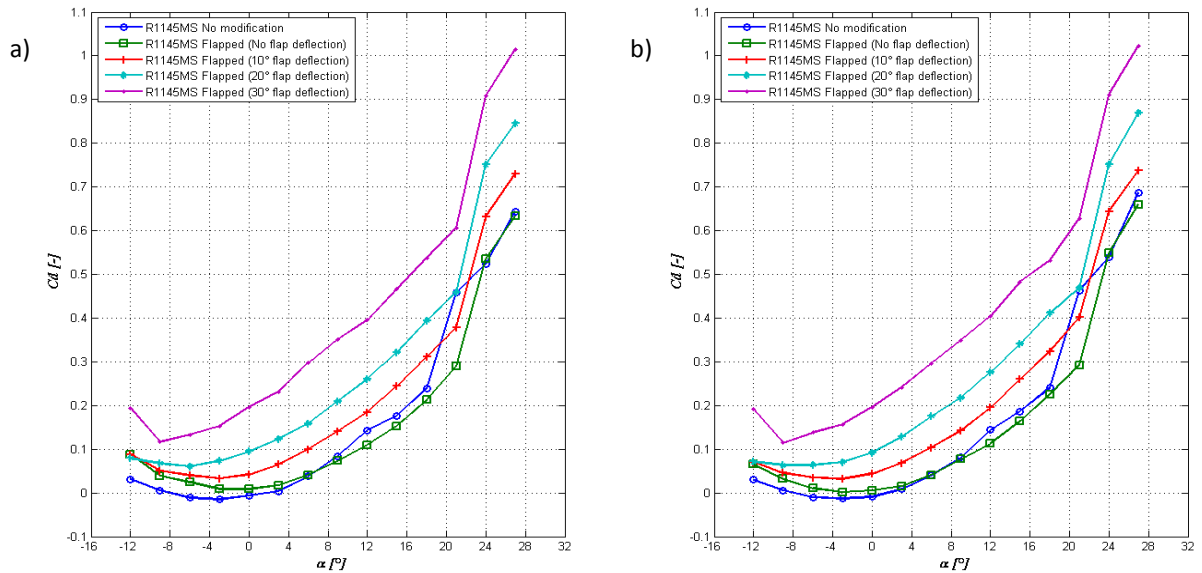


Fig. 5-8 Drag curve R1145MS airfoil at Reynolds: a) 233000 and b) 335000

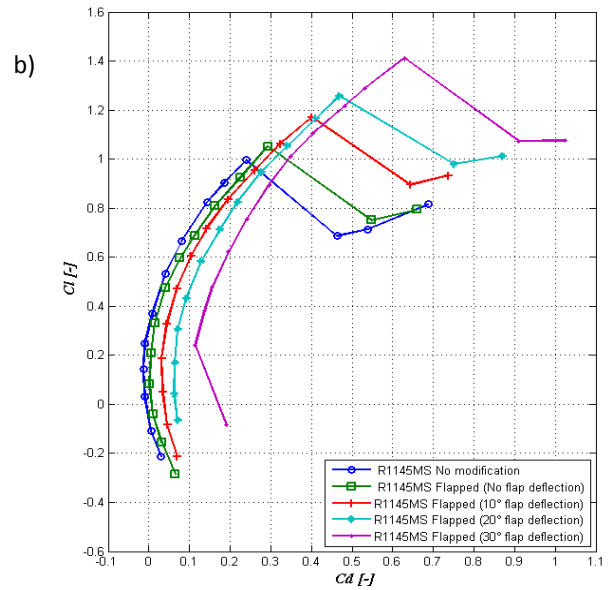
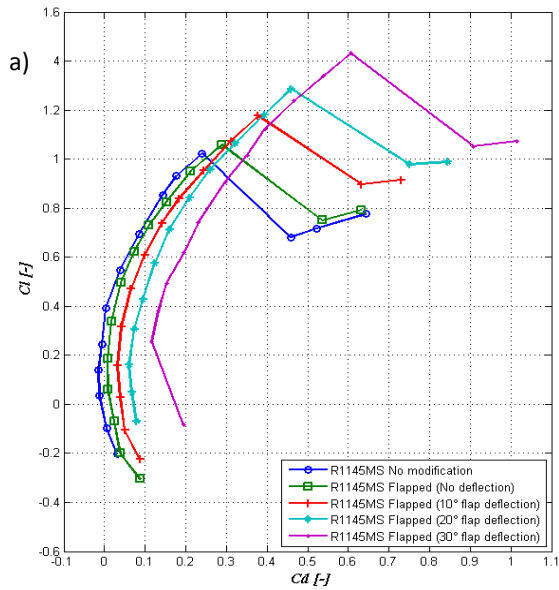


Fig. 5-9 Drag Polar R1145MS airfoil at Reynolds: a) 233000 and b) 335000

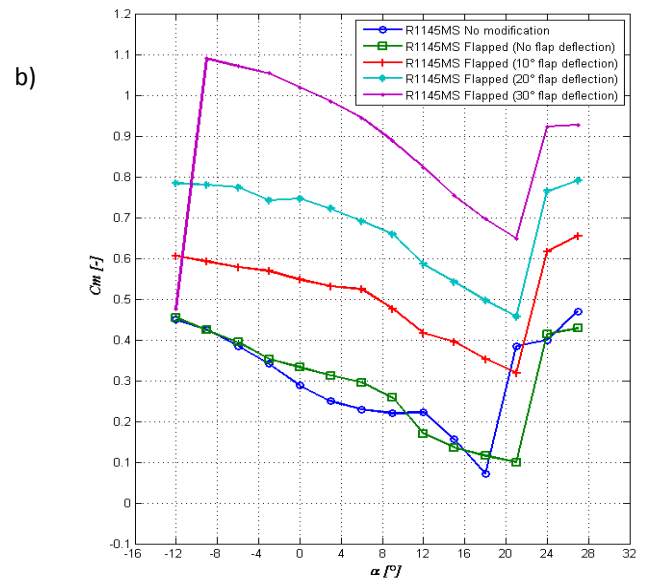
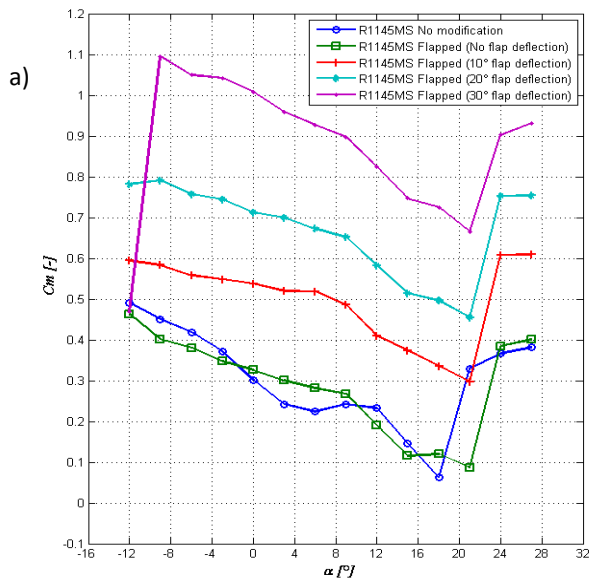


Fig. 5-10 Moment curve R1145MS airfoil at Reynolds: a) 233000 and b) 335000

- Eppler 1230 plots:

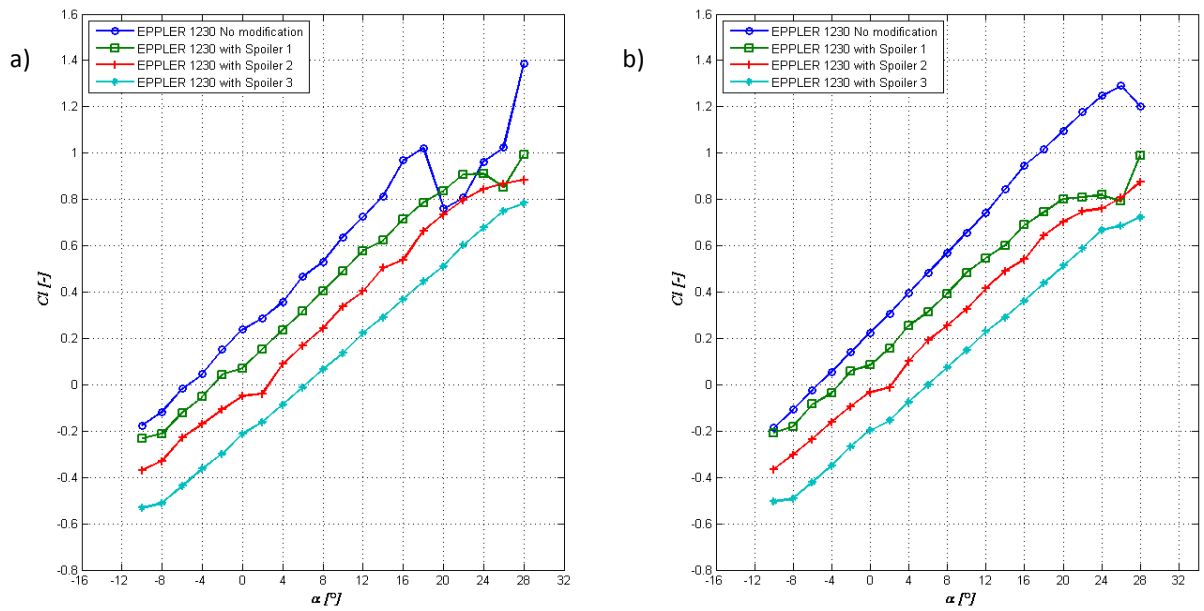


Fig. 5-11 Lift curve Eppler 1230 airfoil at Reynolds: a) 233000 and b) 335000

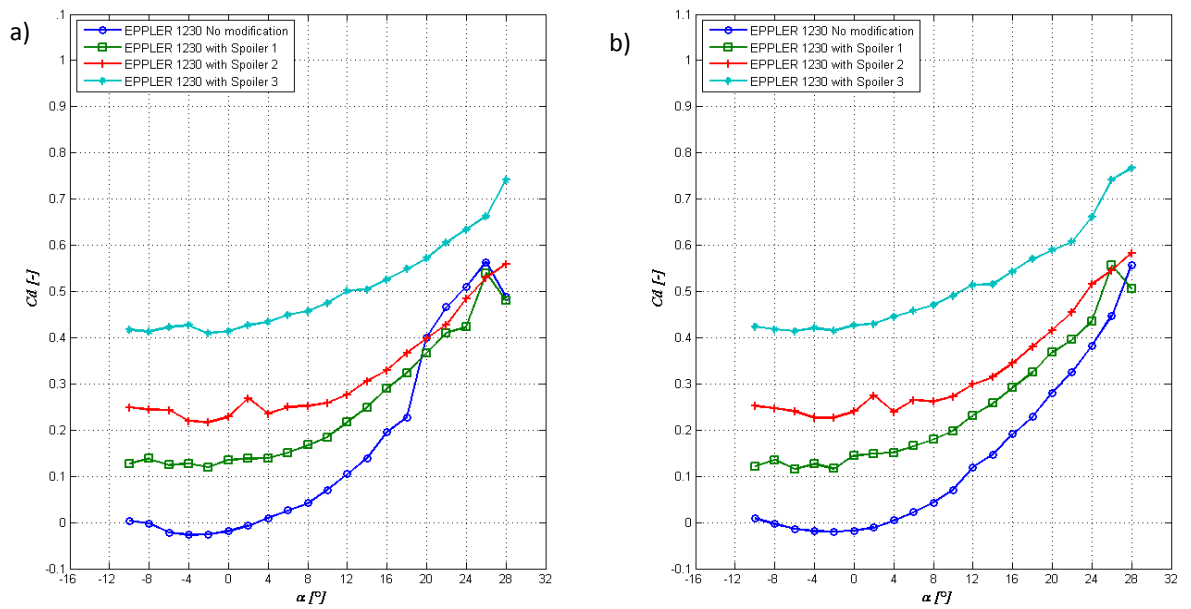


Fig. 5-12 Drag curve Eppler 1230 airfoil at Reynolds: a) 233000 and b) 335000

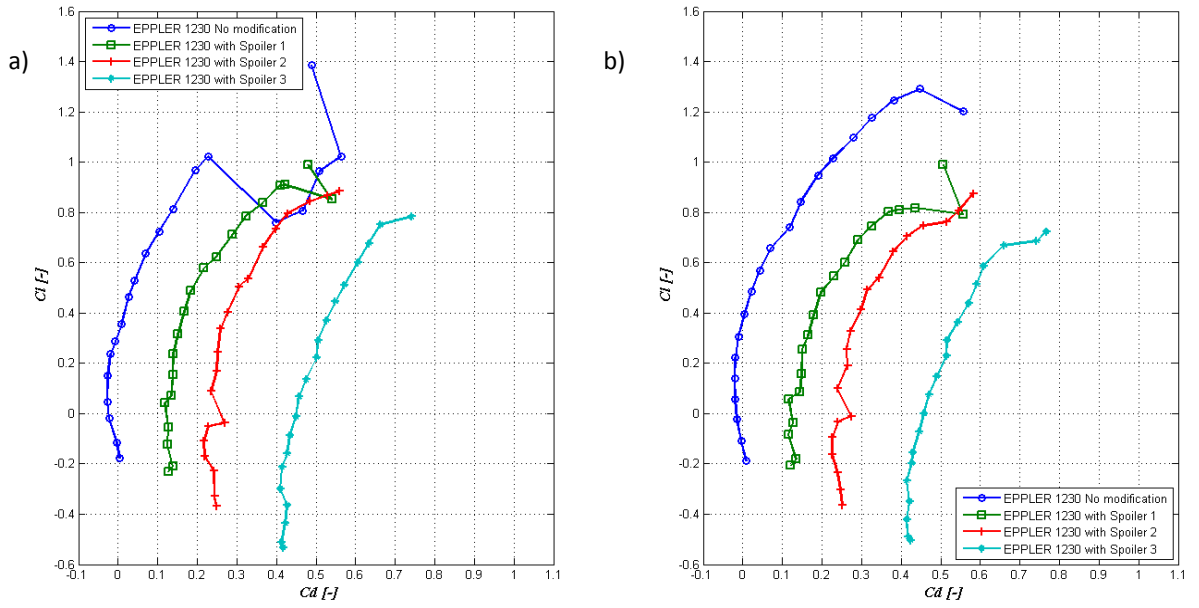


Fig. 5-13 Drag polar Eppler 1230 airfoil at Reynolds: a) 233000 and b) 335000

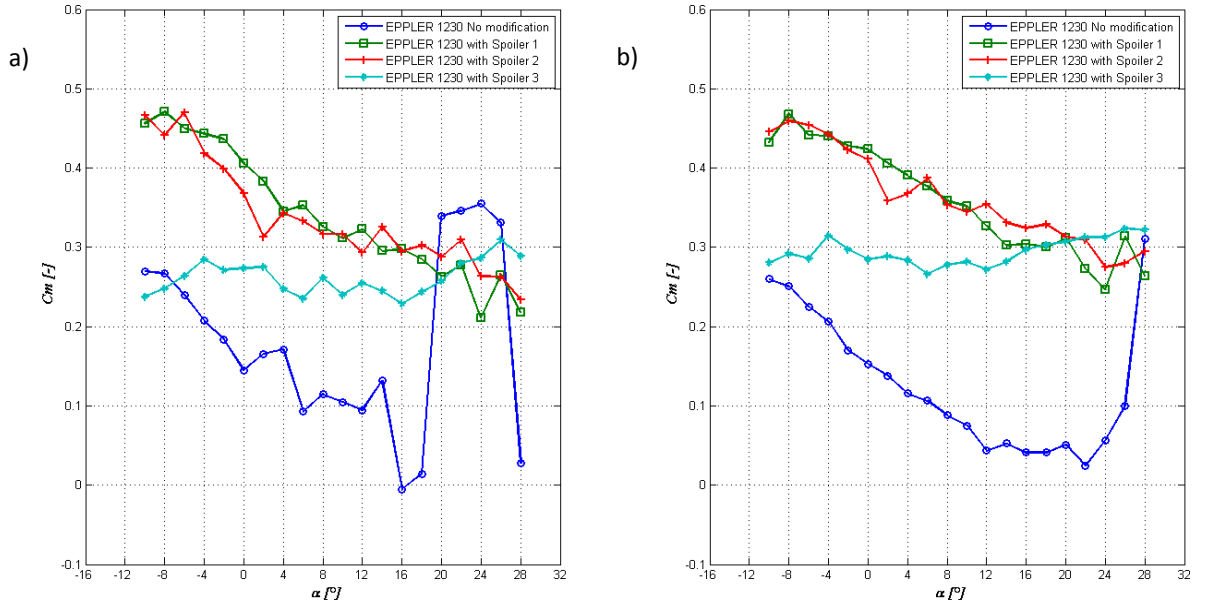


Fig. 5-14 Moment curve Eppler 1230 airfoil at Reynolds: a) 233000 and b) 335000

6. ANALYSIS AND DISCUSSION

A flap is a device intended to increase the lift of the airfoil. Initially, it's noticeable the fact that the data obtained on the R1145MS airfoil for both Reynold's numbers are quite similar. A lift decrease is seen between the non-modified R1145MS and the R1145MS flapped with no flap deflection. It can be addressed to the gap generated by the cuts made on the original airfoil. A clear lift increase is visible for all flap deflections, which was expected according the theory. Nevertheless, α_{stall} is not decreased. This behavior might be generated by the small gap between the flap and the main element of the airfoil allowing the flow of high pressure air from the lower surface into the upper surface. The value of α_{OL} is made more negative as expected, although in the case of -10° flap deflection it remains similar. The drag increases as the flap deflection increases and there is a negative drag for the unmodified airfoil, which is a clear error on the used correction for drag scales.

The purpose of the spoilers is to decrease the lift of the wing. Data obtained from the Eppler 1230 airfoil measurements clearly show the lift decrease, with its minimum for the spoiler 3. The consequently increase in drag caused by the lift decrease is clear too, however, a negative drag for the unmodified airfoil arises once again.

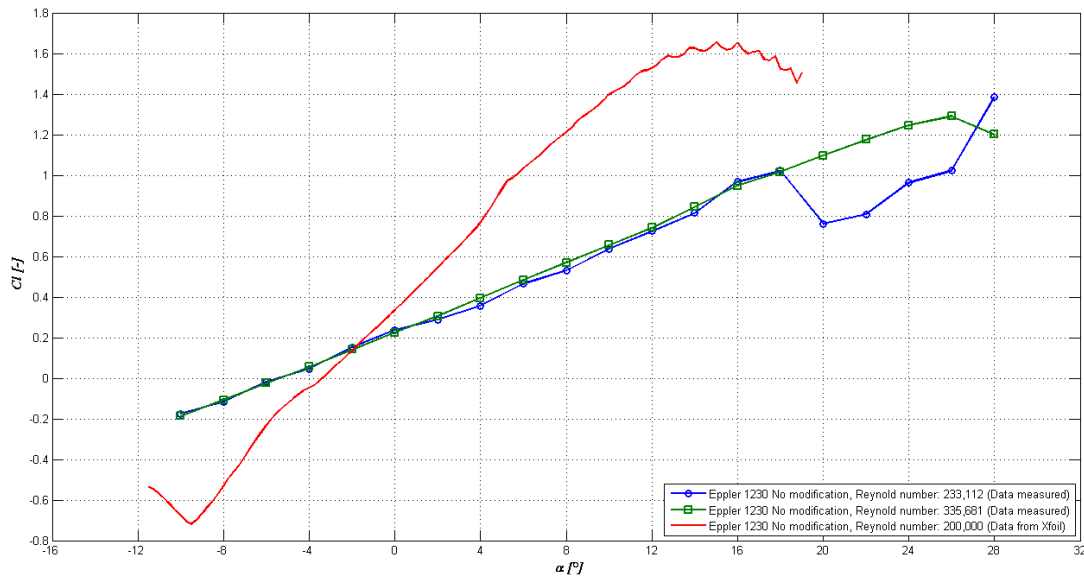


Fig. 6-1 Comparison lift curve

The computed data for the unmodified Eppler 1230 airfoil was downloaded from [19]. Comparison graphs are plotted in order to see how close to expectation (calculated results) the measurement was. The lift curves show a qualitative similar behavior, but the quantitative one is highly different. The measured data gives a lower lift curve, higher α_{stall} and a more negative α_{OL} in comparison to the downloaded Xfoil data. The drag curves also

do not match quantitatively with the Xfoil data.

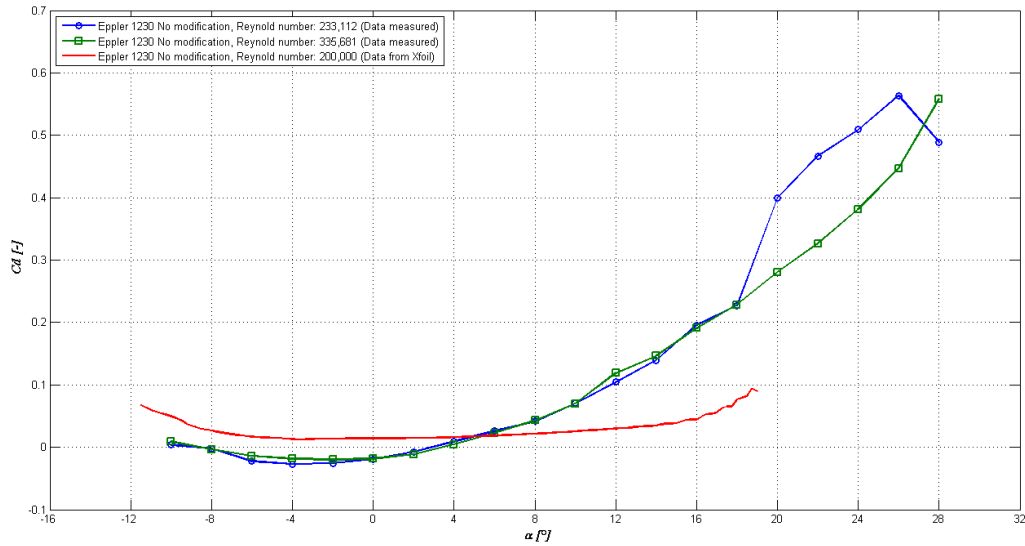


Fig. 6-2 Comparison drag curve

The measured data allows to quantitatively determine the influence of both spoilers and flaps on an airfoil, although the measurement loaded with high error due to the methodology of the experiment. The first factor affecting drag results (slightly negative drag for small part of the drag curve for unmodified airfoil) is the superimposing of the bodies' drag used for eliminating the drag of the scales, which is not a correct assumption. Then, as a high Reynold's number was aimed for in order to obtain more useful and relevant data, due to small test section a low aspect ratio wing had to be tested and even though end plates were used to simulate an infinite wing and reduce the induced drag, these plates were not big enough to eliminate the vortices. Due to low aspect ratio, the boundary layer of the end plates also affected the measurement. If a high aspect ratio wing would have been implemented for the measurements, there would be a problem because of low Reynold's number with all the difficulties connected to low Reynold's number airfoil measurement. Also the manufacturing of the flaps would be difficult.

Although using a relatively large wing in a small test section would require heavy correction (typical corrections are not available for such a big ratio of the wing surface to the wind tunnel's test section opening) for all the mentioned effects affecting results, it was possible to observe the expected influence of the wing mechanization with a greater precision, since the aerodynamic scales are equipped with a relatively large capacity load cells.

7. CONCLUSION

This bachelor thesis was aimed to determine the influence of spoilers and flaps on standard airfoils. In order to summarize the basics of wing geometry, a literature research was carried out. Geometric properties of a wing were briefly covered and later on the cause of a wing's behavior, that is, the aerodynamic forces on a wing, for instance, drag and lift, were covered. The components of drag and the cause of both lift and drag were explained together with the fundamental diagrams reflecting all the aerodynamic properties of a flying body. The last step to achieve the targeted goal was the wind tunnel measurement. Scale models of the Eppler 1230 and R1145MS airfoils were manufactured and put into an open test section wind tunnel, varying the angle of attack, flap deflections and spoilers, to get the final results that were then analyzed, discussed and compared with calculated data.

It was quantitatively proved through the obtained data that the set-up chosen to carry out the measurement is sufficient for understanding the influence of the mechanization of a wing with either spoilers or flaps. These results should not be used without further correction as a trustable source of data for a 2D airfoil (i.e., lift curve, drag curve, drag polar). Even though end plates were used to simulate an infinite wing, the results turned out to be closer to the behavior of a finite wing.

On the other hand, the effects caused by the use of spoilers could be easily measured, contrary to the case in which it would be calculated. The process of calculation of separated flow behind the spoiler is rather complicated. The obtained data allowed the plotting of qualitatively good data which can be further used to design another methodological approach to achieve a quantitatively more reliable and applicable output.

At this concluding step of the bachelor thesis I can say that all the expectations I had before starting this work have been met.

8. BIBLIOGRAPHY

- [1] Kundu, A. (2010). Aircraft design. Cambridge: Cambridge University Press.
- [2] Asselin, M. (1997). An introduction to aircraft performance. Reston, Va, USA.: American Institute of Aeronautics and Astronautics.
- [3] Kroes, M., Rardon, J. and Nolan, M. (2013). Aircraft basic science, eighth edition. [New York]: McGraw-Hill.
- [4] Obert, E., Slingerland, R., Leusink, D., Berg, T., Koning, J. and Tooren, M. (2009). Aerodynamic design of transport aircraft. Amsterdam, the Netherlands: Ios Press.
- [5] Anderson, J. (2000). Introduction to flight, fourth edition. New York: McGraw-Hill.
- [6] Hall, N. (2015). Wing Geometry Definitions. [ONLINE] available at: <http://www.grc.nasa.gov/WWW/k12/airplane/geom.html>. [Accessed April 15]
- [7] Anderson, D. and Eberhardt, S. (2009). Understanding flight, Second edition. New York: McGraw-Hill.
- [8] Nicolai, L., Carichner, G. and Nicolai, L. (2010). Fundamentals of aircraft and airship design. Reston, VA: American Institute of Aeronautics and Astronautics.
- [9] Brandt, S. (2004). Introduction to aeronautics: A Design Perspective, second Edition. Reston, Va.: American Institute of Aeronautics and Astronautics.
- [10] Flandro, G., McMahon, H. and Roach, R. (2012). Basic aerodynamics. Cambridge: Cambridge University Press.
- [11] Federal Aviation Administration (Faa), (2014). Aviation maintenance technician handbook—airframe, volume 1. Aviation Supplies & Academe.
- [12] Kuethe, A. and Chow, C. (1998). Foundations of aerodynamics, fifth edition. New York: Wiley. Foundations of aerodynamics. 5th edition. Arnold M. Kuethe. Chuen-Yen Chow.
- [13] Shevell, R. (1989). Fundamentals of flight, second edition. Englewood Cliffs, N.J.: Prentice-Hall.
- [14] Anderson, J. (1999). Aircraft performance and design. Boston: WCB/McGraw-Hill.
- [15] Anderson, J. (2010). Fundamentals of aerodynamics, fifth edition. Boston: McGraw-Hill.
- [16] Houghton, E., Carpenter, P., Collicott, S. and Valentine, D. (2012). Aerodynamics for engineering students, sixth edition. Oxford: Butterworth-Heinemann.
- [17] Mashud, M., Ferdous, M., Ome, S. (2006). Effect of spoiler position on aerodynamic characteristics of an airfoil. Pakistan: International Journal of Mechanical & Mechatronics Engineering IJMME-IJENS Vol:12 No:06. [ONLINE] Available at: http://www.ijens.org/vol_12_i_06/120306-0707-ijmme-ijens.pdf. [Accessed June 15].

-
- [18] Sadraey, M. Spoiler design. [ONLINE] Available at: <http://faculty.dwc.edu/sadraey/Spoiler%20design.pdf>. [Accessed June 15].
- [19] EPPLER 1230 AIRFOIL (e1230-il). [ONLINE] Available at: <http://airfoiltools.com>. [Accessed April 15].
- [20] Zimčik, L. (2012). Polar diagram measurement. Prague: Czech Technical University in Prague.
- [21] (2000). Canard aviation forum. [ONLINE] Available at: <http://forum.canardaviation.com>. [Accessed April 15]
- [22] AUTOCAD. (2013). Autodesk.
- [23] MATLAB R2013a. (2013). Mathworks.